Human Molecular Genetics, 2011, Vol. 20, No. 9 ***1751–1762***
doi:10.1093/hmg/ddr050
Advance Access published on February 8, 2011

Selective deletion of long but not short Cypher isoforms leads to late-onset dilated cardiomyopathy

Hongqiang Cheng[1,†], Ming Zheng[1,3,†], Angela K. Peter[1], Kensuke Kimura[1], Xiaodong Li[1], Kunfu Ouyang[1], Tao Shen[1,2], Li Cui[1], Derk Frank[4], Nancy D. Dalton[1], Yusu Gu[1], Norbert Frey[4], Kirk L. Peterson[1], Sylvia M. Evans[1,2], Kirk U. Knowlton[1], Farah Sheikh[1] and Ju Chen[1,*]

[1]Department of Medicine and [2]Skaggs School of Pharmacy and Pharmaceutical Sciences, Department of Medicine, University of California San Diego, 9500 Gilman Drive, La Jolla, CA 92093 USA, [3]Institute of Molecular Medicine, Peking University, Beijing 100871, People's Republic of China and [4]Department of Cardiology and Angiology, University Hospital Schleswig-Holstein, Campus Kiel, Schittenhelmstr. 12, 24105 Kiel, Germany

Received January 4, 2011; Revised and Accepted February 3, 2011

Cypher long (CypherL) and short (CypherS) isoforms are distinguished from each other by the presence and absence of three C-terminal LIM domains, respectively. Cypher isoforms are developmentally regulated, and mutations affecting both long and short isoforms are linked to muscle disease in humans. Given these data, we hypothesized that various Cypher isoforms play overlapping and unique roles in striated muscle. To determine the specific role of Cypher isoforms in striated muscle, we generated two mouse lines in which either CypherS or CypherL isoforms were specifically deleted. Mice specifically, deficient in CypherS isoforms had no detectable muscle phenotype. In contrast, selective loss of CypherL isoforms resulted in partial neonatal lethality. Surviving mutants exhibited growth retardation and late-onset dilated cardiomyopathy, which was associated with cardiac fibrosis and calcification, leading to premature adult mortality. At a young age, preceding development of cardiomyopathy, hearts from these mutants exhibited defects in both Z-line ultrastructure and specific aberrations in calcineurin–NFAT and protein kinase C pathways. Earlier onset of cardiac dilation relative to control wild-type mice was observed in young CypherL isoform knockout mice consequent to pressure overload, suggesting a greater susceptibility to the disease. In summary, we have identified unique roles for CypherL isoforms in maintaining Z-line ultrastructure and signaling that are distinct from the roles of CypherS isoforms, while highlighting the contribution of mutations in the long isoforms to the development of dilated cardiomyopathy.

INTRODUCTION

Cypher is a member of the PDZ–LIM domain family and directly complexes with Z-line-associated proteins, such as α-actinin-2 (1–5), thus playing a critical role in muscle ultrastructure and function by maintaining Z-line integrity during muscle contraction in multiple species including mouse, zebrafish and *Drosophila* (3,6–9). The functional importance of Cypher is evidenced by the phenotype of global Cypher-null mice, which are postnatal lethal with severe defects in striated muscle, including a congenital form of dilated cardiomyopathy (10). In addition to its developmental roles, Cypher also plays a critical role in the adult heart, as cardiac-specific deletion in mice causes a severe form of dilated cardiomyopathy resulting in premature adult lethality (11). Importantly, >15 mutations of ZASP, the human Cypher ortholog, have been identified in patients with cardiomyopathies including dilated cardiomyopathy and skeletal muscle myopathies (specifically termed zaspopathy) (7,12–20). However, the underlying molecular basis as to how deficiencies in Cypher lead to striated muscle diseases has not yet been fully understood.

We have previously shown that Cypher exists as six alternatively spliced isoforms that can be characterized as cardiac or skeletal muscle specific (21). Cardiac and skeletal muscle each contain two long isoforms, which have three C-terminal LIM domains and may have a signaling role in addition to a structural role at the Z-line, and one short isoform without

*To whom correspondence should be addressed. Tel: +1 8588224276; Fax: +1 8588221355; Email: juchen@ucsd.edu
†The authors wish it to be known that, in their opinion, the first two authors should be regarded as joint First Authors.

LIM domains, which is primarily localized to the Z-line (21). Similarly, human ZASP exists as six alternatively spliced isoforms, analogous to those in mouse striated muscle (13). Expression of both long and short Cypher isoforms is tightly regulated during muscle development (21). For example, Cypher short (CypherS) isoforms (2c, 2s) are barely detectable during embryogenesis but are strikingly induced postnatally in both cardiac and skeletal muscles (21). In contrast, Cypher long (CypherL) isoforms (1c, 1s, 3c, 3s) exhibit consistent expression patterns from embryonic stages to adulthood (21). Functionally unique roles for CypherS isoforms in muscle disease have also been suggested by specific early loss of CypherS isoforms along with calsarcin-1 in enigma homolog (ENH)-null hearts, which exhibit dilated cardiomyopathy (22). These studies suggest that short and long Cypher isoforms could have both overlapping and unique roles in muscle development and disease.

In humans, a ZASP mutation (R268C) that affects only short isoforms is associated with skeletal myopathies (18), while ZASP mutations (I352M, D626N, T350I D366N, Y468S, Q519P, P615L) that affect only long isoforms are primarily associated with cardiomyopathies, some of which affect specific signaling pathways such as protein kinase C (PKC) (7,12,13,23,24). These findings indicate that isoform-specific mutations in ZASP may result in distinct etiologies of muscle disease; however, the underlying molecular and signaling mechanisms remain unclear.

By generating two novel CypherS and CyperL isoform-specific knockout mouse models, we sought to further determine isoform-specific roles of Cypher in striated muscle function and disease. Our present studies demonstrated that CypherS isoform knockout (CypherS KO) mice developed no detectable phenotypic abnormalities in muscle. In contrast, CypherL isoform knockout (CypherL KO) mice displayed partial neonatal lethality. Surviving CypherL KO mice exhibited growth retardation and late-onset dilated cardiomyopathy associated with early and selective defects in Z-line ultrastructure, as well as signaling [increased calcineurin–NFAT and specific PKC (α, β and ε)] pathways. These studies identify unique roles for CypherL isoforms in Z-line ultrastructure and in signaling that are distinct from the roles for CypherS isoforms. Additionally, our data provide insights into mechanisms by which mutations in CypherL isoforms are causative in muscle diseases, such as dilated cardiomyopathy.

RESULTS

Generation of CypherS and CypherL isoform-specific knockout mice

To investigate the specific role of CypherS and CypherL isoforms in regulating striated muscle function and disease, both CypherS (Cypher 2c, 2s) and CypherL (Cypher 1c, 3c, 1s and 3s) isoform-specific knockout mouse lines were generated by floxing exons 10 and 12 of the *cypher* gene, respectively (Fig. 1A and D), based on our previous studies (21). Southern blot analyses of DNA isolated from G418-resistant embryonic stem (ES) cells identified wild-type (WT) (+/+) as well as targeted CypherS (f/+) and CypherL (f/+) floxed alleles (Fig. 1B and E). Western blot analysis demonstrated that deletion of exons 10 and 12 successfully targeted the deletion of CypherS and CypherL isoforms, respectively, in CypherS and CypherL KO mouse hearts (Fig. 1C and F). However, loss of one Cypher isoform reciprocally affects the expression of the other Cypher isoform as evidenced by the increased expression of CypherL and CypherS isoforms in CypherS and CypherL KO mouse hearts, respectively (Fig. 1C and F).

Early postnatal growth retardation and late-onset dilated cardiomyopathy in CypherL but not CypherS KO mice

CypherS and CypherL KO mice were born at expected Mendelian ratios; however, only 72% of CypherL KO mice survived until the age of 3 weeks (Table 1), with most of the mortality observed within the first week after birth (Fig. 2A). Analysis of surviving CypherL KO mice during the first 3 weeks after birth revealed that these mice displayed dramatic growth retardation when compared with WT littermates, as reflected by significantly smaller body size (Fig. 2B) and lower body weight (Fig. 2C). Growth defects observed in CypherL KO mice gradually lessened with age and allowed these mice to reach body weights similar to those of WT littermates by 3 months of age (Fig. 2D). However, CypherL KO mice subsequently displayed a premature adult mortality, beginning at 16 months, with none surviving past 20 months of age (Fig. 2A). Serial echocardiographic assessment of CypherL KO mouse hearts revealed late-onset cardiomyopathy, beginning at 9 months, which was suggestive of dilated cardiomyopathy. CypherL KO mouse hearts were characterized by significant increases in chamber size [increased left ventricular internal dimensions at end-diastole (LVIDd)] at 9 months of age and significant chamber wall thinning [decreased left ventricular posterior wall thickness at end-diastole (LVPWd)], which reached statistical significance at 16 months (a time point when sudden death was observed) when compared with WT littermate hearts (Fig. 2E and F). The heart weight to body weight (HW/BW) ratio of CypherL KO mouse hearts was also significantly increased at 9 months when compared with WT controls (Fig. 2G). Fractional shortening (FS), an index of left ventricle systolic function, also progressively and significantly decreased with age in CypherL KO mice, reaching lows of 20% by 16 months (Fig. 2H). When compared with WT littermates, no significant differences in cardiac dimensions and function could be observed in CypherL KO hearts at 5 months of age (Fig. 2E–G). It should also be noted that CypherS KO mice did not display any differences in cardiac dimensions and function up to 2 years of age when compared with WT controls, when assessed by echocardiography (Supplementary Material, Fig. S1).

Histological assessment of CypherL KO hearts revealed left and right ventricular chamber enlargement at 9 months when compared with WT controls, which was not apparent at 5 months (Fig. 3A), which is consistent with our findings using echocardiography (Fig. 2E–G). CypherL KO hearts exhibited severe fibrosis (Fig. 3B) and calcification (Fig. 3C) at 5 months, the latter of which could be readily visualized by aberrant densities of brightness using echocardiography. Echocardiography revealed that ~38% of CypherL KO hearts displayed calcification (data not shown). CypherL KO

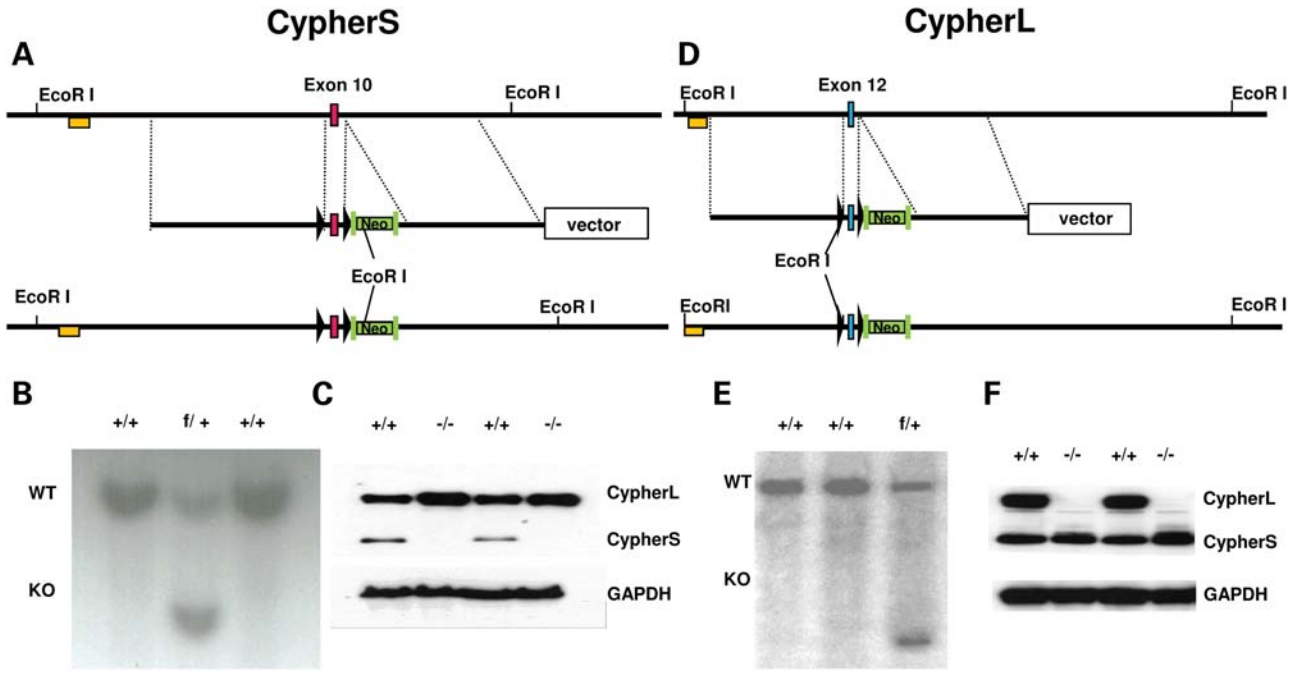

Figure 1. Targeted deletion of CypherS and CypherL isoforms in mice. (**A**, **D**) Genomic region of interest for CypherS (exon 10) and CypherL (exon 12) (top), the targeting construct for CypherS and CypherL isoforms where Cypher exons 10 and 12 (red box) are floxed by two *LoxP* sites (black triangles), respectively, and contain a neomycin cassette (Neo) flanked by two *FRT* sites (green rectangle) inserted into introns 10 and 12 for CypherS and CypherL, respectively (center), and the floxed locus for CypherS and CypherL after homologous recombination (bottom). (**B**, **E**) DNA from G418-resistant ES cells was digested with the restriction enzyme *Eco*RI and analyzed by Southern blotting for WT (+/+) and targeted (f/+) alleles for CypherS and CypherL isoforms with probes (yellow box) as shown in A and D, respectively. (**C**, **F**) Protein from WT, CypherS (C) and CypherL (F) isoform knockout mouse hearts was subjected to immunoblotting to detect the expression of CypherS and CypherL. GAPDH was used to normalize for protein loading.

Table 1. Genotypes of offspring at 3 weeks of age from heterozygous CypherL$^{+/-}$ (or CypherS$^{+/-}$) intercrosses to show partial postnatal lethality of CypherL KO mice

	CypherL Number	Percentage (%)	CypherS Number	Percentage (%)
Total (female:male)	261 (129:132)		102 (52:50)	
WT (female:male)	75 (44:31)	28.7	26 (11:15)	25.5
KO (female:male)	47 (18:29)	18	26 (13:13)	25.5
Heterozygous (female:male)	137 (64:73)	52.5	50 (28:22)	49

hearts also displayed significant increases in the expression of the cardiac fetal gene markers atrial natriuretic factor and skeletal α-actin as early as 6 weeks of age, when compared with WT controls, consistent with early molecular changes in cardiac stress preceding histological/functional defects leading to the development of dilated cardiomyopathy. Interestingly, changes in the expression of fetal gene markers could not be detected in CypherL KO hearts at 3 weeks (data not shown) or in CypherS KO hearts up to 2 years of age (Supplementary Material, Fig. S2).

Young CypherL KO hearts display susceptibility to cardiac dilation/enlargement following biomechanical stress

To determine potential cues that could lead to the late-onset dilated cardiomyopathy in CypherL KO mice, we subjected young CypherL KO mice to biomechanical (2 months of age) or β-adrenergic stress (3 months of age) via pressure overload and chronic isoproterenol stimulation, respectively. Both young CypherL KO and WT mice displayed an increase in cardiac chamber wall thickness (LVPWd) 2 and 4 weeks following transverse aortic constriction (TAC), consistent with a hypertrophic response (Fig. 4A). However, young CypherL KO mice also uniquely displayed a significant increase in chamber wall dimensions (LVIDd) associated with an impairment in cardiac function (FS%) when compared with WT hearts following TAC (Fig. 4B and C). Interestingly, young CypherS KO mice subjected to TAC did not exhibit significant changes compared to WT hearts (Supplementary Material, Fig. S3). Chronic isoproterenol stimulation of young CypherL KO mice also led to significant and aberrant increases in the LV/BW (left ventricle weight/body weight) ratio (Fig. 4D), when compared with WT mice, further demonstrating an increased susceptibility of CypherL KO mice to adverse changes in cardiac dimensions and function.

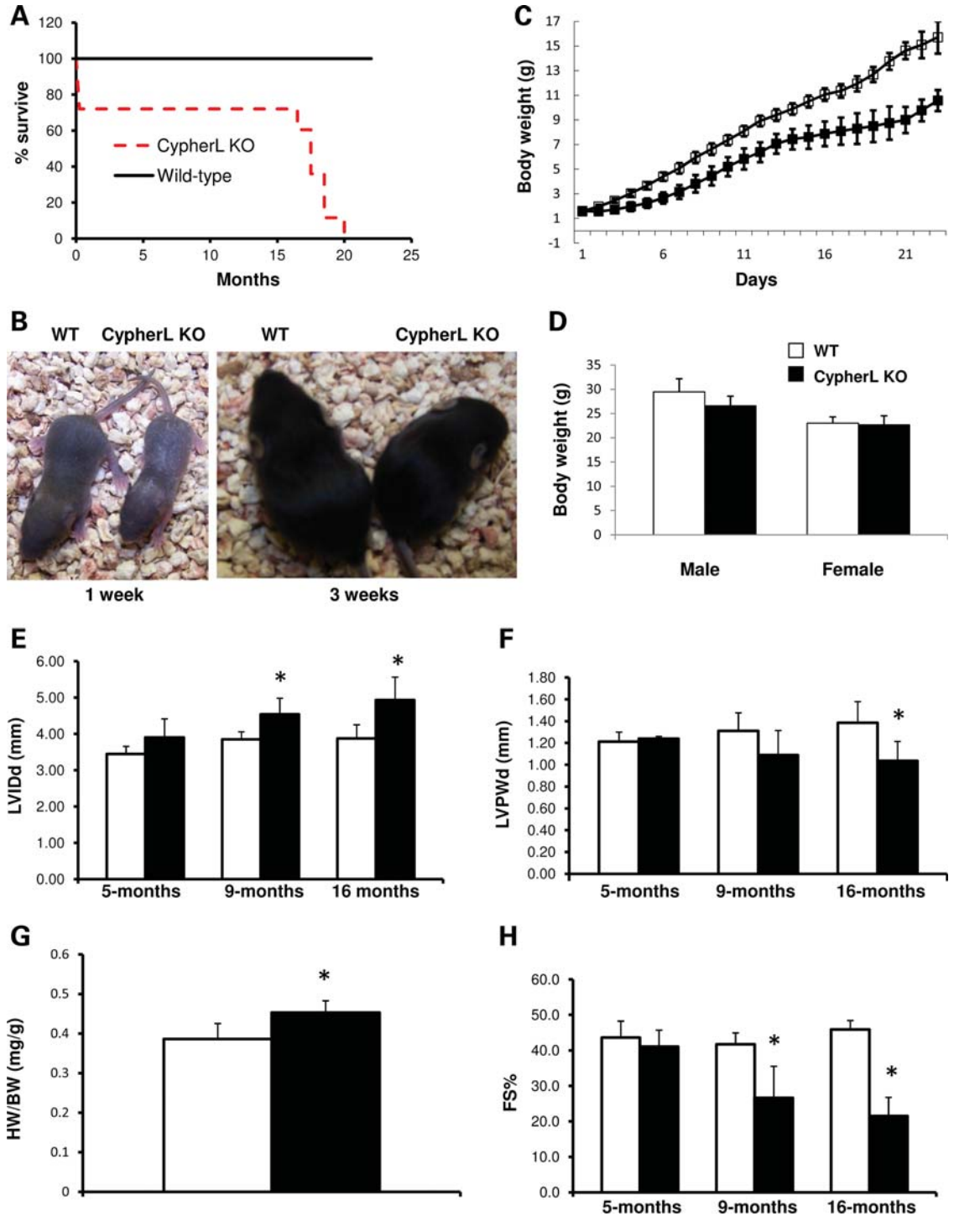

Figure 2. Growth retardation, dilated cardiomyopathy and premature lethality in CypherL KO mice. (**A**) Partial lethality (28%) in CypherL KO mice was observed in the first week after birth. Of the surviving mice, premature lethality was observed in CypherL KO mice beginning at the age of 16 months. In contrast to WT control mice, no CypherL KO mice survived longer than 20 months. (**B**) Representative pictures show the smaller body size of CypherL KO mice at the age of 1 and 3 weeks. (**C**) The body weight of CypherL KO mice ($n = 4$) at the first 3 weeks after birth was dramatically smaller than that of WT controls ($n = 7$). (**D**) Both male and female CypherL KO mice displayed normal body weights beginning at 3 months. (**E**–**H**) Dilated cardiomyopathy in CypherL KO mice assessed by echocardiography ($n = 6$ for each group). (E) Enlarged left ventricle chambers of CypherL KO mice as measured by echocardiography was significant beginning at the age of 9 months. (F) Left ventricle wall thickness in CypherL KO mice was significantly less at 16 months. (G) The ratio of heart weight to body weight (HW/BW) (mg/g) was larger in CypherL KO mice ($n = 8$) than in WT controls ($n = 7$) at 9 months. (H) CypherL KO mice displayed dramatically reduced heart function as shown by FS% beginning at 9 months progressing in severity until the age of 16 months ($^*P < 0.05$).

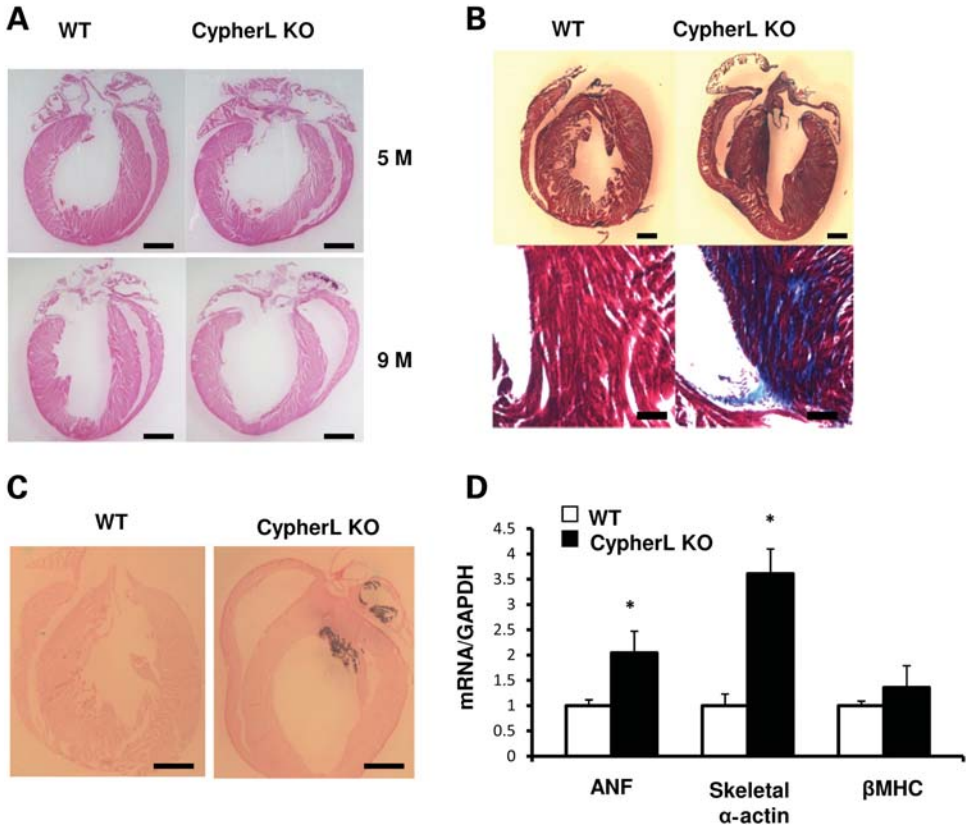

Figure 3. Characterization of dilated cardiomyopathy in CypherL KO mice. (**A**) Representative morphology of WT and CypherL KO mouse hearts at the age of 5 and 9 months after H&E staining. Both chambers of the CypherL KO heart are dilated at the age of 9 months. The scale bars are 1 mm. (**B**) Fibrosis was found at 5 months in CypherL KO mouse hearts by Masson's trichrome stain. The scale bars are 1 mm for the top and 100 μm for the bottom. (**C**) Calcification at 5 months in CypherL KO mouse hearts as shown by Von Kossa staining. The scale bars are 1 mm. (**D**) mRNA levels for cardiac fetal genes (ANF, atrial natriuretic factor; β-MHC and skeletal α-actin) was quantified and normalized to GAPDH from the densities of dot-blot analysis of 6-week-old CypherL KO and WT mouse hearts. GAPDH was used as an RNA loading control ($^*P < 0.05$).

Inotropic and lusitropic dysfunction precedes dilated cardiomyopathy in CypherL KO mice

To further explore contractile defects in CypherL KO hearts, we subjected 5-month-old WT and CypherL KO mice to cardiac hemodynamic evaluation at rest and following stepped increases in dobutamine (β-adrenergic) stimulation. Heart rates and left ventricle peak systolic pressure (either at baseline or when stimulated with various doses of dobutamine) were not significantly different between CypherL KO and WT mice (Fig. 5A and B). However, when stimulated with 4 μg/kg/min of dobutamine, CypherL KO mice exhibited significant contractile dysfunction as evidenced by a decreased maximum positive derivative of LV pressure as measured over time (Max dP/dt) (Fig. 5C). Furthermore, the minimum positive derivative of LV pressure as measured over time (Min dP/dt, at baseline and when stimulated with various concentrations of dobutamine) was significantly reduced in CypherL KO mice, when compared with WT mice (Fig. 5D). Additionally, the calculated tau values, using a linear regression fit of the relation between dP/dt and pressure during isovolumic pressure decline, were significantly longer in CypherL KO than in WT mice (Fig. 5E). Altogether, these data indicate that CypherL KO mice developed early inotropic and lusitropic dysfunction at 5 months of age before the onset of histological/functional defects associated with dilated cardiomyopathy. In contrast, CypherS KO mice demonstrated no differences in systolic or diastolic function at 2 years of age either at basal conditions or under various concentrations of dobutamine stimulation, when compared with WT littermate mice (Supplementary Material, Fig. S4).

CypherL but not CypherS KO mice display underlying cardiac muscle Z-line abnormalities

Since Cypher directly localizes to the Z-line (10,11), we performed transmission electron microscopy (TEM) to examine the ultrastructure of the Z-line in left ventricular cardiomyocytes of young CypherL KO mice at 3 months of age (Fig. 6). We demonstrate that CypherL KO cardiomyocytes displayed dramatically wider Z-lines (473.1 ± 132.7 versus 84.9 ± 9.1 nm; $P \leq 0.001$; CypherL KO versus WT, respectively), which were also disorganized (Fig. 6A–C) when compared with WT cardiomyocytes. M-line structure was lost in areas where there was severe disruption in cardiac muscle Z-line architecture in CypherL KO hearts (Fig. 6B). Interestingly, we could also identify regions in CyperL KO hearts with intact Z-line integrity and organized sarcomeric structure as seen in WT cardiac muscle (data not shown), suggesting a

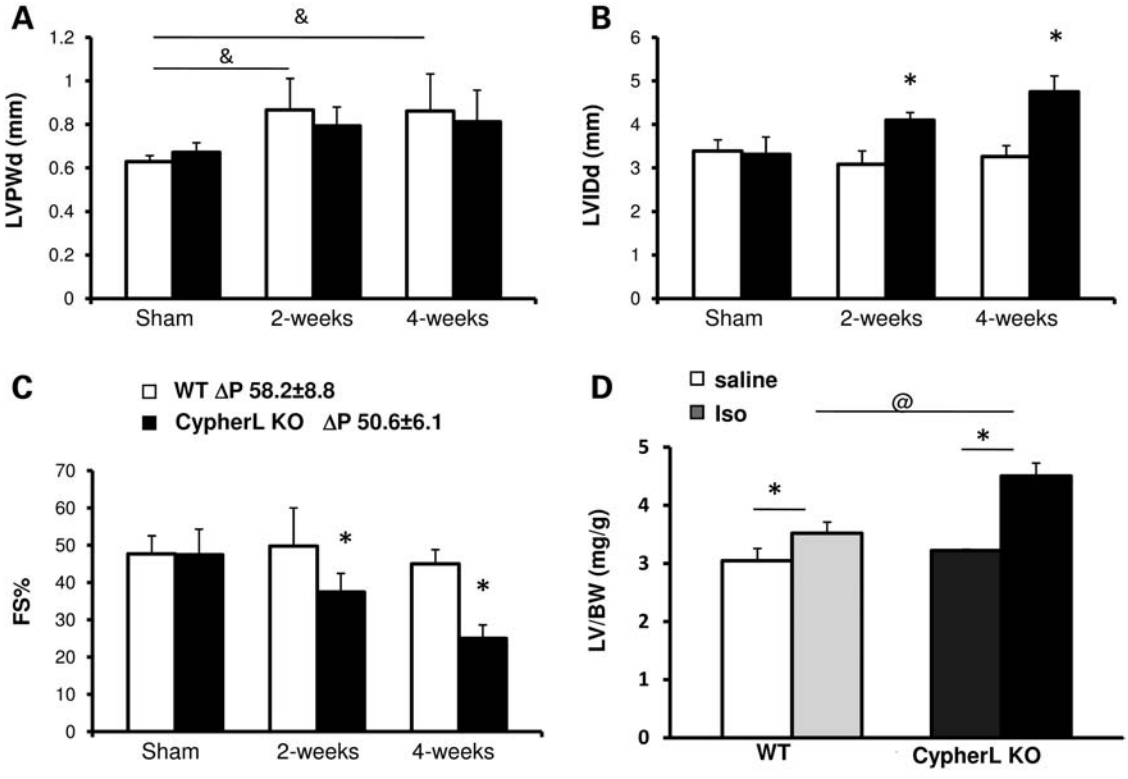

Figure 4. Stress-induced dilated cardiomyopathy in young CypherL KO mice. (**A**) CypherL KO and WT mice had comparable hypertrophic responsiveness 2 and 4 weeks post-TAC surgery as shown by left ventricular posterior wall thickness (LVPWd) at end-diastole assessed by echocardiography ($^{\&}P < 0.05$ between sham and TAC groups). (**B**) CypherL KO mice developed dilated left ventricles 2 and 4 weeks post-TAC surgery ($^{*}P < 0.05$ between WT and CypherL KO). (**C**) Reduced heart function in CypherL KO mice 2 or 4 weeks post-TAC surgery as shown by FS% ($^{*}P < 0.05$ between WT and CypherL KO). (**D**) Increased hypertrophic responsiveness in CypherL KO mouse hearts after 1 week chronic isoproterenol treatment was shown by increased left ventricular mass ($^{*}P < 0.05$ between saline and isoproterenol treatments; $^{@}P < 0.05$ between WT and CypherL KO with treatment).

level of heterogeneity in Z-line ultrastructural defects at this age. Sarcomere lengths in cardiac muscles of CypherL KO mice were comparable with those of WT controls (data not shown). No detectable defects in cardiac sarcomeric ultrastructure were observed in CypherS KO hearts at this age, when compared with WT littermate hearts (Supplementary Material, Fig. S5).

CypherL KO hearts display aberrant expression of specific protein complexes associated with Z-line ultrastructure and signaling

To determine the influence of CypherL isoform ablation on the expression of other Z-line-associated proteins, we assessed expression levels of proteins thought to either directly (myotilin, calsarcin-1, PKC, α-actinin-2, ENH) or indirectly (desmin, αB-crystallin, calcineurin) bind to Cypher at the Z-line, in relatively young CypherL KO hearts, prior to the dilated phenotype. Overall, no significant differences in cytoskeletal proteins, α-actinin and desmin, were observed in CypherL KO hearts when compared with controls (Fig. 7A). However, a significant upregulation in Z-line-associated proteins, myotilin and αB-crystallin, was seen in CypherL KO hearts (Fig. 7A). As previously demonstrated, a compensatory increase of CypherS isoforms was observed in CypherL KO hearts. CypherS isoforms are thought to directly interact/form a complex with ENH and calsarcin-1 at the Z-line (22); however, no significant differences in ENH isoforms or calsarcin-1 were observed in CypherL KO hearts when compared with WT controls (Fig. 7A). Interestingly, a significant increase in the activity of the calsarcin-1-interacting protein, calcineurin, was observed in CypherL KO hearts prior to the dilated phenotype. This was evidenced by an increase in nuclear translocation of NFATc4 (Fig. 7B and C), a substrate of calcineurin, as well as an increase in mRNA and protein levels of MCIP, a downstream target of NFAT, in CypherL KO hearts, when compared with WT controls (Fig. 7D and E).

CypherL, but not CypherS, isoforms also directly bind to various PKC isoforms through their C-terminal LIM domains (1). We found that expression of PKCα, β and ε but not PKCδ was significantly upregulated in CypherL KO hearts when compared with WT controls (Fig. 8A and B) prior to the dilated phenotype. No detectable difference in expression of PKCs was observed in CypherS KO mouse hearts when compared with WT controls (Supplementary Material, Fig. S6). To determine the specificity of signaling pathways affected via ablation of Cypher isoforms, we assessed the expression of several other growth-related signaling pathways in CypherL KO hearts. Similar to our previous report of the cardiac-specific deletion of Cypher, we found no detectable changes in the activation of Akt in CypherL KO mouse hearts when compared with WT controls

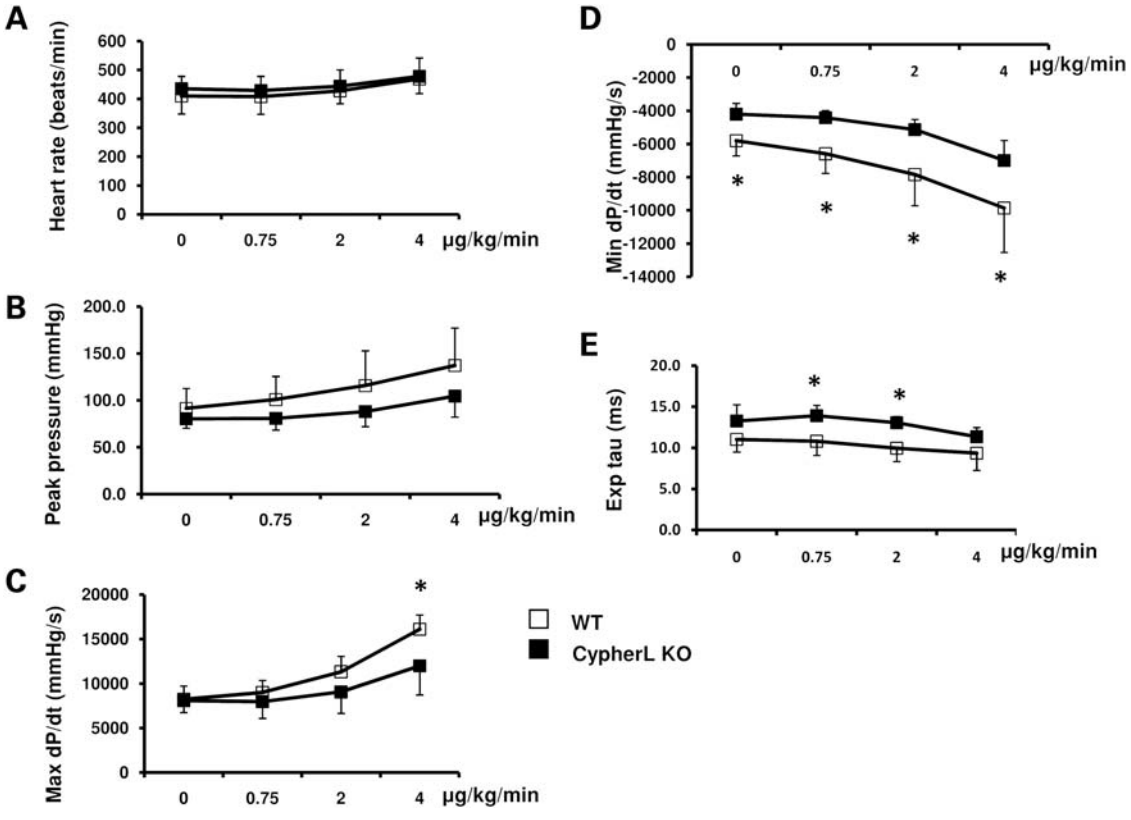

Figure 5. Impaired contractility in CypherL KO mouse hearts. (**A** and **B**) WT and CypherL KO mice had comparable heart rates and left ventricle systolic blood pressure at the age of 5 months. (**C**) CypherL KO mice had significantly reduced maximum d*P*/d*t* under 4 ug/kg/min of dobutamine stimulation. (**D**) CypherL KO mice have reduced minimum d*P*/d*t* both at basal condition and with various doses of dobutamine perfusion. (**E**) Tau was larger in CypherL KO mice under 0.75 or 2 µg/kg/min of dobutamine stimulation than WT control mice ($^*P < 0.05$).

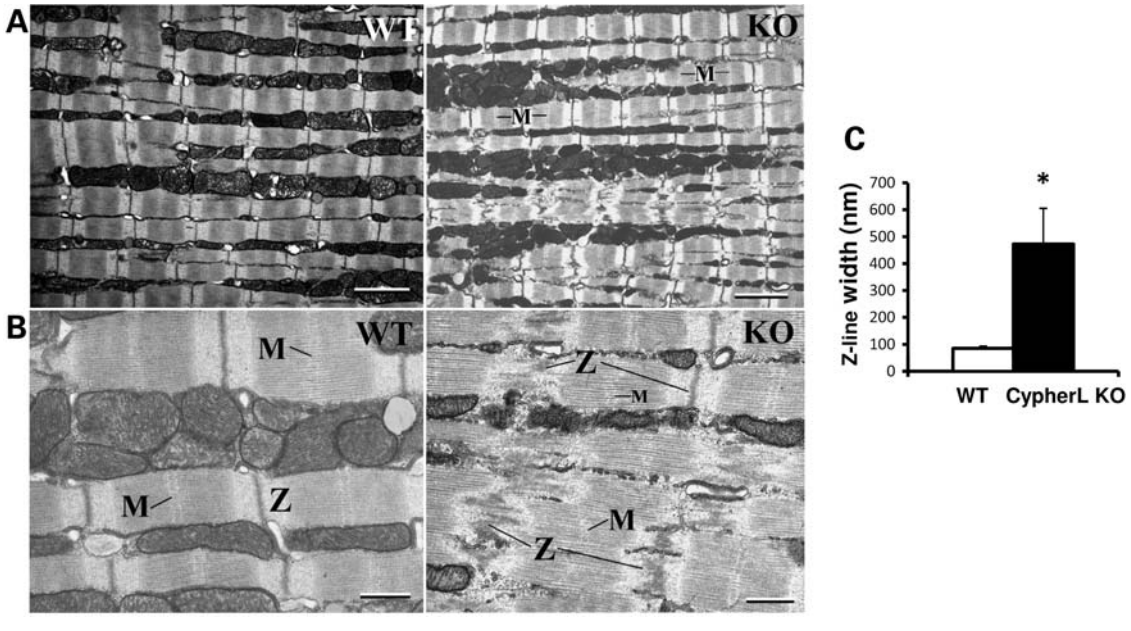

Figure 6. Disorganized Z-lines in CypherL KO mouse cardiac muscle. Representative transmission electron microscopy (TEM) pictures showed the sarcomeric structure of cardiac muscle from 3-month-old male mice depicting disorganized Z-lines in a CypherL KO mouse when compared with normal Z-lines in WT controls. (**A**) Low magnification with bars: 1 µm. (**B**) High magnification with bars: 500 nm. (**C**) Width of Z-lines for WT and CypherL KO (abnormal Z-lines only) ($^*P < 0.05$).

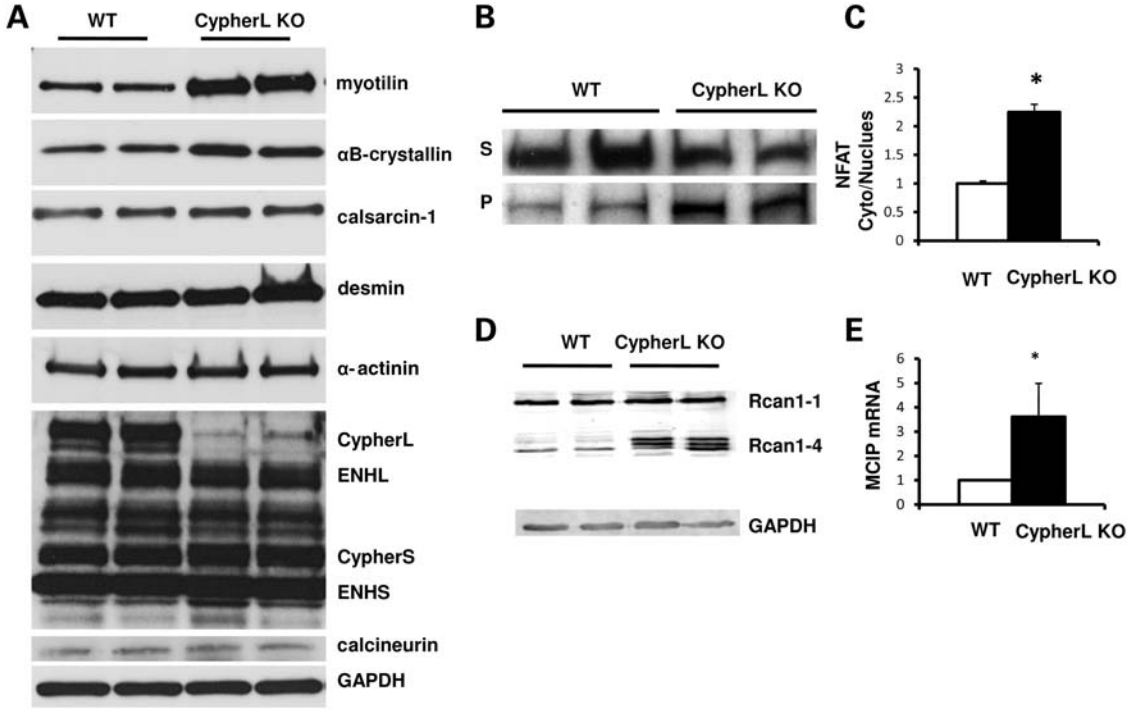

Figure 7. Immunoblotting of Z-line and Z-line-associated proteins and activated NFAT–calcineurin pathway in CypherL KO hearts. (**A**) The expression of myotilin and αB-crystallin was increased in CypherL KO hearts, while the expression of α-actinin, desmin, calsarcin-1, calcineurin and enigma homolog (ENH) was not altered in CypherL KO mouse hearts. (**B**, **C**) NFATc4 protein translocated from the cytosol to the nucleus as shown by western blot in CypherL KO hearts. The densities were quantified and normalized to WT controls ($^*P < 0.05$). (**D**, **E**) Modulatory calcineurin-interacting protein, MCIP, a gene directly targeted by NFATcs, was upregulated at both the protein and mRNA levels in CypherL KO hearts ($^*P < 0.05$). GAPDH was used as protein loading control.

(Fig. 8C). In contrast to the Cypher cardiac-specific KO hearts, neither Erk1/2 nor P38 mitogen-activated protein kinase (MAPK) phosphorylation was significantly altered in 3-month-old CypherL KO mouse hearts when compared with WT controls (Fig. 8C), further demonstrating the specificity of Z-line protein signaling complexes affected by ablation of CypherL isoforms.

We also found that filamin C, which connects to the Z-line via myotilin and calsarcin and to the membrane via the dystrophin–glycoprotein complex, and βID integrin were significantly upregulated in CypherL KO hearts. In addition, various components of the dystrophin–glycoprotein complex, including syntrophin and γ-sarcoglycan, were also upregulated in CypherL KO hearts (Fig. 8D) prior to the onset of dilated cardiomyopathy. In CypherS KO mouse hearts, with the exception of myotilin and dystrophin, whose expression was slightly increased, all other Z-line-associated proteins and members of the dytrophin–glycoprotein complex were unaltered (Supplementary Material, Fig. S6), highlighting a specific connection between CypherL/Z-line and the sarcolemma–sarcoglycan complex.

DISCUSSION

Cypher is known to interact with multiple protein complexes at the Z-line, including α-actinin, myotilin, calsarcin-1 and PKC (1,11,25). However, specific interactions of individual Cypher isoforms with distinct Z-line protein signaling complexes, and the relevance of these interactions to human disease remain unclear. Utilizing isoform-specific Cypher-deficient mice, we provide direct evidence for a unique role for CypherL isoforms in cardiac Z-line protein signaling/structural complexes which is critical for Z-line ultrastructural integrity. Loss of CypherL isoforms leads to late-onset dilated cardiomyopathy. We also define two developmental stages where CypherL but not short isoforms are essential for survival, as evidenced by the significant postnatal lethality exhibited by 28% of CypherL KO mice, similar to conventional Cypher-null mice in which all Cypher isoforms are ablated (10), and the adult lethality caused by late-onset dilated cardiomyopathy exhibited in CypherL KO mice, similar to cardiac-specific Cypher KO mice (11). Despite upregulated expression of CypherS in CypherL KO mice, these mice develop late-onset dilated cardiomyopathy with fibrosis and calcification, as well as early susceptibility to cardiomyopathy following biomechanical stress.

Our studies suggest that CypherS isoforms are dispensable for mouse survival, cardiac muscle development and the response to cardiac stress. However, in contrast to global knockout mice in which all Cypher isoforms are ablated and where all mice die within the first week after birth (10), some CypherL mutants survive until adulthood, suggesting some degree of functional overlap between CypherL and CypherS isoforms. This is consistent with our previous studies, which demonstrated that either long or short Cypher

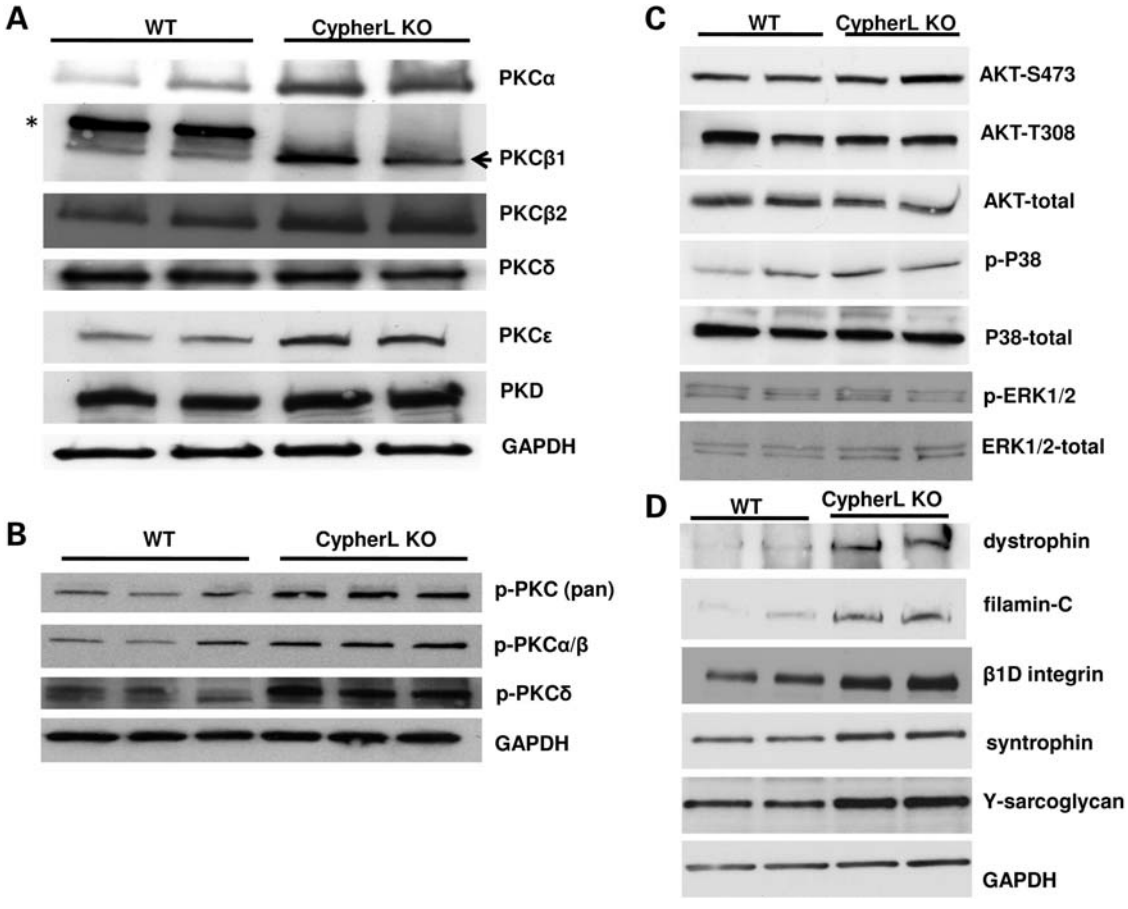

Figure 8. Activation of PKC pathways and no alteration in the activities of AKT and MAPK pathways. (**A**) The expression of PKCα, β and ε was specifically increased in CypherL KO mouse hearts. (**B**) The activation of PKCα/β and δ was increased in CypherL KO mouse hearts as shown by immunoblotting using phospho-specific antibodies. (**C**) No difference in the activation of AKT, ERK, P38 and JNK was shown by immunoblotting analyses. (**D**) The expression of β1D-integrin, filamin C and members of the dystrophin–glycoprotein complex including dystrophin, syntrophin and γ-sarcoglycan was increased in CypherL KO mouse hearts.

skeletal isoforms (Cypher1s or Cypher2s) can partially rescue the lethal phenotype of Cypher-null mice (21). It should be pointed out that all mouse models utilized for these studies were in the same mixed 129/SvJ and Black Swiss background. Whether genetic background plays a role in the observed partial neonatal lethality and late-onset cardiomyopathy of CypherL mutants has yet to be determined.

Cypher plays an important role in the integrity of Z-line ultrastructure (10,11). However, the role of specific Cypher isoforms in maintaining Z-line structural integrity remains unclear. The current studies have demonstrated that CypherL but not CypherS KO hearts display widened and disorganized Z-lines in adult cardiac muscle, which suggests that the short isoforms do not play a structural role in maintaining Z-line integrity, or that the short isoforms in CypherL KO hearts are not sufficient to maintain intact Z-lines in cardiac muscle. CypherL and CypherS isoforms contain a common PDZ domain, which recognizes the C-terminus of α-actinin-2, calsarcin-1 and myotilin, and a ZM motif that recognizes the rod-domain of α-actinin-2 (1,11,25,26). Our results suggest that interactions between Cypher and α-actinin-2 may not be sufficient to maintain the integrity of the Z-line. Since only CypherL KO hearts displayed disorganized Z-line structures, our studies further suggest that there remain novel interactions between CypherL and potentially the unique Cypher LIM domains and other Z-line proteins that are critical to maintenance of Z-line integrity.

Cypher can interact with a number of Z-line-associated proteins; however, the relevant Z-line-associated protein interactions underlying Z-line defects observed in CypherL KO mice remain unclear. We showed, through protein analyses, that young CypherL KO hearts displayed specific increases in two major Z-line-associated protein signaling complexes, highlighting CypherL isoforms as a nodal point for Z-line signaling. The calcineurin–NFAT pathway was aberrantly activated in young CypherL KO hearts, as evidenced by increased NFATc4 nuclear translocation and expression of MCIP, a downstream target of NFAT (27,28), in CypherL but not CypherS KO hearts, prior to the onset of the dilated phenotype. Calcineurin is a phosphatase that can interact with calsarcin-1 at the Z-line (29–31) and is thought to play an important role in cardiac hypertrophy and dilated cardiomyopathy (32–35). We and others have also shown that Cypher can interact with calsarcin-1 through its PDZ

domain (11,25), identifying a Cypher/calsarcin-1/calcineurin complex that could be critical in maintaining Z-line integrity/signaling and contributing to the pathogenesis of dilated cardiomyopathy. Although our studies suggest that Cypher may negatively regulate calcineurin activity within this complex, our data clearly demonstrate that the observed effects on calcineurin activity are independent of alterations to calsarcin-1, since loss of CypherL isoforms does not alter levels of calsarcin-1 in CypherL KO hearts.

Our studies also reveal that PKCα, β and ε signaling pathways are aberrantly and selectively activated in CypherL but not CypherS KO mouse hearts, prior to the onset of the dilated phenotype. We have previously demonstrated that the long isoforms of Cypher directly interact with PKC isoforms (α, β, ζ, γ, δ and ε) via their LIM domains, and can be phosphorylated by PKCs (1). Accumulating evidence suggests that PKC signaling plays a critical role in the development of cardiac hypertrophy (36–38). *In vivo* models of pressure overload hypertrophy and human heart failure are associated with increased activity of a number of PKC isoforms (39–41). In addition, overexpression of PKCβII in mouse heart results in hypertrophy and cardiomyopathy (42), while overexpression of PKCε results in the development of dilated cardiomyopathy with heart failure (43,44). Studies in human patients with Cypher/ZASP mutations identified a particular gain-of-function mutation within the Cypher/ZASP third LIM domain (D626N) that is causative for dilated cardiomyopathy and enhances the affinity of PKC for Cypher/ZASP (12). The current studies suggest the possibility that CypherL isoforms (and LIM domains) uniquely act to negatively regulate PKC signaling in the normal heart.

Our studies further highlight Z-line protective mechanisms essential for optimal force generation and transmission, which are activated within the CypherL KO heart, prior to the onset of dilated cardiomyopathy. We specifically demonstrate upregulation of αB-crystallin, a stress protein associated with Z-lines, as well as increases in myotilin, filamin C and components of the integrin/dystrophin–glycoprotein complex in CypherL KO hearts, prior to the onset of the dilated phenotype. These alterations are likely to result in compensatory increased connections between sarcomeres and the extracellular matrix, suggestive of Z-line protection. Since increased myotilin and dystrophin were also observed in CypherS KO hearts, our studies have identified both unique and overlapping molecular pathways consequent to the mutations of distinct Cypher isoforms, some of which are important for susceptibility to cardiomyopathy.

In conclusion, the present study has demonstrated unique and essential roles for CypherL isoforms in survival as well as its roles in Z-line ultrastructure, signaling [e.g. calcineurin–NFAT and PKC (α, β and ε) pathways] and function in adult cardiac muscle, which are different from those of CypherS isoforms. Our studies provide mechanistic insight into mechanisms by which mutations in CypherL isoforms result in muscle diseases, such as dilated cardiomyopathy. We believe that these studies pave the way to a better understanding of Cypher isoforms in striated muscle function *in vivo*, which could also be of critical importance in screening and treating different types of muscle pathologies.

MATERIALS AND METHODS

Generation of two Cypher isoform-specific KO mouse models

Genomic DNA fragments specific for *cypher* short (exon 10) or long (exon 12) isoforms were amplified from mouse ES cells (129/SvJ) using polymerase chain reaction (PCR) and used to construct both CypherS and CypherL targeting constructs, as previously described (Fig. 1) (45). For the CypherS construct, one *LoxP* site was inserted into intron 9 and a second *LoxP* site together with a neomycin cassette flanked by *FRT* sites was inserted into intron 10. For the CypherL construct, the first *LoxP* site was inserted into intron 11 and the second *LoxP* site with a neomycin cassette was inserted into intron 13. Both targeting vectors were linearized with the restriction enzyme *Not*I and electroporated into R1 ES cells derived from 129/SvJ mice (UCSD Transgenic and Gene Targeting Core, La Jolla, CA, USA). Homologous recombinants of both constructs were identified by Sothern blotting. Genomic DNA from G418-resistant ES cell clones was digested with the restriction enzyme *Eco*RI and hybridized with the radiolabeled 453-bp 5′-probes as indicated in Figure 1. The WT allele is represented as a 17.1 kb band, whereas a 4.2 kb band represents the targeted allele. All fragments generated by PCR using high-fidelity KOD Hot Start DNA polymerase (Novagen, Gibbstown, CA, USA) were cloned into the PCR-Blunt II-TOPO vector (Invitrogen, Carlsbad, CA, USA), and sequences were verified.

Two independent homologous recombinant clones for either the CypherS or CypherL constructs were microinjected into C57BL/6 blastocysts. Male chimeras were bred with female Black Swiss mice (Taconic Inc., Hudson, NY, USA) to generate germline-transmitted heterozygous mice with a neo cassette ($CypherS^{fneo/+}$ or $CypherL^{fneo/+}$), which were further confirmed by PCR and Southern blot analysis of mouse tail DNA. Following confirmation, the neomycin cassette flanked by two *FRT* sites was removed ($CypherS^{f/+}$ or $CypherL^{f/+}$) by crossing a floxed heterozygous mouse ($CypherS^{fneo/+}$ or $CypherL^{fneo/+}$) with an FLPe transgenic mouse as previously described (46). Heterozygous mice ($CypherS^{+/-}$ or $CypherL^{+/-}$) were obtained by crossing targeted mice ($CypherS^{f/+}$ or $CypherL^{f/+}$) with the protamine-Cre transgenic mouse line as previously described (47). Heterozygous mice were interbred to generate homozygous KO mice ($CypherS^{-/-}$ or $CypherL^{-/-}$). Offspring were genotyped by PCR with the following primer sets: for CypherS, WT primers (P1, 5′-GCTTCTCTCTGGAGG TGGTG-3′ and P2, 5′-GCTTTGGCAGTAGGCTCTTG-3′) and mutant allele primers (P1 and P4, 5′-CCTTGCTGGAA GGAAAGGTA-3′); for CypherL, WT primers (P1, 5′-TC CTCCCCTATTTGGCTTCTTTCT-3′and P2, 5′-CTGGAACC AAGGCAGAAGAG-3′); mutant allele primers (P5, 5′-CCA CAGTCCTACTGCTACATTCTG-3′ and P6 5′-TCCAGCT AGGACTATCTGTTTCCT-3′). All procedures described in this manuscript were completed using mice of a mixed 129/SvJ and Black Swiss background.

All procedures were performed in accordance with the NIH *Guide for the Care and Use of Laboratory Animals* and approved by the Institutional Animal Care and Use Committee of UCSD.

Echocardiography and hemodynamic measurement

Adult mice were anesthetized with 1% isoflurane and subjected to echocardiography as previously described (22). Adult mice were anesthetized using 100 mg/kg ketamine and 5 mg/kg xylazine and subjected to hemodynamic measurement as described previously (22).

RNA analysis

Total RNA was isolated from mouse ventricles using Trizol reagent (Invitrogen) following the manufacturer's protocol. RNA dot-blot and real-time PCR were performed as previously described (22). Quantitation of RNA levels from the dot-blot result was performed using ImageJ software. The oligonucleotide primers for MCIP used for real-time PCR were as follows: forward: 5′-TCCAGCTTGGGCTTGACTGAG-3′ and reverse: 5′-ACTGGAAGGTGGTGTCCTTGTC-3′.

Transmission electron microscopy

TEM was performed as described previously at the National Center for Microscopy and Imaging Research, University of California San Diego (22).

Histological analysis

Hematoxylin and eosin (H&E) staining was performed on 7-μm sections according to standard procedures (10). Trichrome staining was performed using the manufacturer's protocol (Sigma, St Louis, MO, USA). Calcification was detected by Von Kossa staining as previously described (48).

Western blot analysis

Freshly isolated hearts were homogenized in RIPA buffer with protease inhibitor cocktail (Roche, Basel, Switzerland) and PhosSTOP (Roche). Protein concentration was determined by DC protein assay kit (BioRad, Hercules, CA, USA). Standard procedures were used for SDS–PAGE and subsequent transfer to PVDF membranes. Filamen-C, myotilin and βID integrin antibodies were gifts from Dr Louis M. Kunkel (Harvard Medical School, Boston, MA, USA), Dr Olli Carpen (University of Helsinki, Helsinki, Finland) and Dr Robert S. Ross (University of California San Diego, La Jolla, CA, USA), respectively. Commercial antibodies for α-actinin (Sigma-Aldrich, St Louis, MO, USA), calsarcin-1 (Alpha Diagnostic International, San Antonio, TX, USA), calcineurin (BD Biosciences, San Jose, CA, USA), desmin, syntrophin (Abcam, Cambridge, MA, USA), αB-crystallin (Stressgen, Ann Arbor, MI, USA), dystrophin (Spring Biosciences, Pleasanton, CA, USA) and γ-sarcoglycan (Vector Laboratories, Burlingame, CA, USA) were used. MAPK, p-MAPK and AKT antibody sampler kits were purchased from Cell Signaling Technologies (Danvers, MA, USA). Antibodies for GAPDH and NFATc4 were purchased from Santa Cruz Biotechnology (Santa Cruz, CA, USA). Antibodies for PKCs were purchased from Cell Signaling Technologies (Danvers) and Santa Cruz. The ENH antibody was purchased from Novus Biologicals (Littleton, CO, USA).

Transverse aortic constriction banding and isoproterenol administration

Two-month-old male mice either underwent a sham operation or were subjected to pressure overload induced by thoracic aorta banding as previously described (22). Echocardiography measurements were performed before surgery, 2 and 4 weeks post-TAC. Mice were sacrificed 4 weeks post-TAC.

For chronic isoproterenol administration, mini-osmotic pumps (model 1007D, Alzet) containing isoproterenol or saline were inserted subcutaneously in the backs of 3-month-old male mice. The pumps delivered either 28 μg of isoproterenol per hour per 25 g of body weight in a 0.9% saline solution or saline alone as a negative control as previously described (49). Mice were sacrificed 7 days later for the assessment of cardiac hypertrophy.

Statistics

All data are expressed as mean values ± standard error of the mean. We performed statistical evaluation using Student's unpaired *t*-test. $P < 0.05$ was considered to be statistically significant.

SUPPLEMENTARY MATERIAL

Supplementary Material is available at *HMG* online.

Conflict of Interest statement. None declared.

FUNDING

This work was supported by grants from the National Institute of Health (J.C., F.S., K.U.K., S.M.E. and P.L.P.) and the Muscular Dystrophy Association (J.C.). F.S. is a recipient of an American Heart Association Scientist Development Grant. A.K.P. was supported by an American Heart Association Postdoctoral Fellowship award. M.Z. was supported by the National Science Foundation of China (30770870 and 30971062) and the National Key Basic Research Program of China (2007CB512108).

REFERENCES

1. Zhou, Q., Ruiz-Lozano, P., Martone, M.E. and Chen, J. (1999) Cypher, a striated muscle-restricted PDZ and LIM domain-containing protein, binds to alpha-actinin-2 and protein kinase C. *J. Biol. Chem.*, **274**, 19807–19813.
2. Velthuis, A.J.W.T. and Bagowski, C.P. (2007) PDZ and LIM domain-encoding genes: molecular interactions and their role in development. *Scientific World Journal*, **7**, 1470–1492.
3. Zheng, M., Cheng, H., Banerjee, I. and Chen, J. (2010) ALP/Enigma PDZ–LIM domain proteins in the heart. *J. Mol. Cell Biol.*, **2**, 96–102.
4. Faulkner, G., Pallavicini, A., Formentin, E., Comelli, A., Ievolella, C., Trevisan, S., Bortoletto, G., Scannapieco, P., Salamon, M., Mouly, V. *et al.* (1999) ZASP: a new Z-band alternatively spliced PDZ-motif protein. *J. Cell Biol.*, **146**, 465–475.
5. Passier, R., Richardson, J.A. and Olson, E.N. (2000) Oracle, a novel PDZ–LIM domain protein expressed in heart and skeletal muscle. *Mech. Dev.*, **92**, 277–284.
6. van der Meer, D.L.M., Marques, I.J., Leito, J.T.D., Besser, J., Bakkers, J., Schoonheere, E. and Bagowski, C.P. (2006) Zebrafish cypher is important for somite formation and heart development. *Dev. Biol.*, **299**, 356–372.

7. Sheikh, F., Bang, M.L., Lange, S. and Chen, J. (2007) "Z"eroing in on the role of Cypher in striated muscle function, signaling, and human disease. *Trends Cardiovasc. Med.*, **17**, 258–262.
8. Jani, K. and Schock, F. (2007) ZASP is required for the assembly of functional integrin adhesion sites. *J. Cell Biol.*, **179**, 1583–1597.
9. Benna, C., Peron, S., Rizzo, G., Faulkner, G., Megighian, A., Perini, G., Tognon, G., Valle, G., Reggiani, C., Costa, R. *et al.* (2009) Post-transcriptional silencing of the *Drosophila* homolog of human ZASP: a molecular and functional analysis. *Cell Tissue Res.*, **337**, 463–476.
10. Zhou, Q., Chu, P.H., Huang, C., Cheng, C.F., Martone, M.E., Knoll, G., Shelton, G.D., Evans, S. and Chen, J. (2001) Ablation of Cypher, a PDZ–LIM domain Z-line protein, causes a severe form of congenital myopathy. *J. Cell Biol.*, **155**, 605–612.
11. Zheng, M., Cheng, H., Li, X., Zhang, J., Cui, L., Ouyang, K., Han, L., Zhao, T., Gu, Y., Dalton, N.D. *et al.* (2009) Cardiac-specific ablation of Cypher leads to a severe form of dilated cardiomyopathy with premature death. *Hum. Mol. Genet.*, **18**, 701–713.
12. Arimura, T., Hayashi, T., Terada, H., Lee, S.Y., Zhou, Q., Takahashi, M., Ueda, K., Nouchi, T., Hohda, S., Shibutani, M. *et al.* (2004) A Cypher/ZASP mutation associated with dilated cardiomyopathy alters the binding affinity to protein kinase C. *J. Biol. Chem.*, **279**, 6746–6752.
13. Vatta, M., Mohapatra, B., Jimenez, S., Sanchez, X., Faulkner, G., Perles, Z., Sinagra, G., Lin, J.H., Vu, T.M., Zhou, Q. *et al.* (2003) Mutations in Cypher/ZASP in patients with dilated cardiomyopathy and left ventricular non-compaction. *J. Am. Coll. Cardiol.*, **42**, 2014–2027.
14. Selcen, D. and Carpen, O. (2008) The Z-disk diseases. *Adv. Exp. Med. Biol.*, **642**, 116–130.
15. Ichida, F. (2009) Left ventricular noncompaction. *Circ. J.*, **73**, 19–26.
16. Ferrer, I. and Olive, M. (2008) Molecular pathology of myofibrillar myopathies. *Expert Rev. Mol. Med.*, **10**, e25.
17. Moric-Janiszewska, E. and Markiewicz-Loskot, G. (2008) Genetic heterogeneity of left-ventricular noncompaction cardiomyopathy. *Clin. Cardiol.*, **31**, 201–204.
18. Selcen, D. and Engel, A.G. (2005) Mutations in ZASP define a novel form of muscular dystrophy in humans. *Ann. Neurol.*, **57**, 269–276.
19. Griggs, R., Vihola, A., Hackman, P., Talvinen, K., Haravuori, H., Faulkner, G., Eymard, B., Richard, I., Selcen, D., Engel, A. *et al.* (2007) Zaspopathy in a large classic late-onset distal myopathy family. *Brain*, **130**, 1477–1484.
20. Arimura, T., Inagaki, N., Hayashi, T., Shichi, D., Sato, A., Hinohara, K., Vatta, M., Towbin, J.A., Chikamori, T., Yamashina, A. *et al.* (2009) Impaired binding of ZASP/Cypher with phosphoglucomutase 1 is associated with dilated cardiomyopathy. *Cardiovasc. Res.*, **83**, 80–88.
21. Huang, C.Q., Zhou, Q., Liang, P.H., Hollander, M.S., Sheikh, F., Li, X.D., Greaser, M., Shelton, G.D., Evans, S. and Chen, J. (2003) Characterization and *in vivo* functional analysis of splice variants of cypher. *J. Biol. Chem.*, **278**, 7360–7365.
22. Cheng, H., Kimura, K., Peter, A.K., Cui, L., Ouyang, K., Shen, T., Liu, Y., Gu, Y., Dalton, N.D., Evans, S.M. *et al.* (2010) Loss of enigma homolog protein results in dilated cardiomyopathy. *Circ. Res.*, **107**, 348–356.
23. Marziliano, N., Mannarino, S., Nespoli, L., Diegoli, M., Pasotti, M., Malattia, C., Grasso, M., Pilotto, A., Porcu, E., Raisaro, A. *et al.* (2007) Barth syndrome associated with compound hemizygosity and heterozygosity of the *TAZ* and *LDB3* genes. *Am. J. Med. Genet. A*, **143A**, 907–915.
24. Theis, J.L., Bos, J.M., Bartleson, V.B., Will, M.L., Binder, J., Vatta, M., Towbin, J.A., Gersh, B.J., Ommen, S.R. and Ackerman, M.J. (2006) Echocardiographic-determined septal morphology in Z-disc hypertrophic cardiomyopathy. *Biochem. Biophys. Res. Commun.*, **351**, 896–902.
25. von Nandelstadh, P., Ismail, M., Gardin, C., Suila, H., Zara, I., Belgrano, A., Valle, G., Carpen, O. and Faulkner, G. (2009) A class III PDZ binding motif in the myotilin and FATZ families binds enigma family proteins: a common link for Z-disc myopathies. *Mol. Cell. Biol.*, **29**, 822–834.
26. Klaavuniemi, T. and Ylanne, J. (2006) Zasp/Cypher internal ZM-motif containing fragments are sufficient to co-localize with alpha-actinin: analysis of patient mutations. *Exp. Cell Res.*, **312**, 1299–1311.
27. Sanna, B., Brandt, E.B., Kaiser, R.A., Pfluger, P., Witt, S.A., Kimball, T.R., van Rooij, E., De Windt, L.J., Rothenberg, M.E., Tschop, M.H. *et al.* (2006) Modulatory calcineurin-interacting proteins 1 and 2 function as calcineurin facilitators *in vivo*. *Proc. Natl Acad. Sci. USA*, **103**, 7327–7332.
28. Molkentin, J.D. (2004) Calcineurin–NFAT signaling regulates the cardiac hypertrophic response in coordination with the MAPKs. *Cardiovasc. Res.*, **63**, 467–475.
29. Frey, N., Barrientos, T., Shelton, J.M., Frank, D., Rutten, H., Gehring, D., Kuhn, C., Lutz, M., Rothermel, B., Bassel-Duby, R. *et al.* (2004) Mice lacking calsarcin-1 are sensitized to calcineurin signaling and show accelerated cardiomyopathy in response to pathological biomechanical stress. *Nat. Med.*, **10**, 1336–1343.
30. Frey, N., Richardson, J.A. and Olson, E.N. (2000) Calsarcins, a novel family of sarcomeric calcineurin-binding proteins. *Proc. Natl Acad. Sci. USA*, **97**, 14632–14637.
31. Frank, D., Kuhn, C., van Eickels, M., Gehring, D., Hanselmann, C., Lippl, S., Will, R., Katus, H.A. and Frey, N. (2007) Calsarcin-1 protects against angiotensin-II induced cardiac hypertrophy. *Circulation*, **116**, 2587–2596.
32. Molkentin, J.D. (2000) Calcineurin and beyond: cardiac hypertrophic signaling. *Circ. Res.*, **87**, 731–738.
33. Molkentin, J.D., Lu, J.R., Antos, C.L., Markham, B., Richardson, J., Robbins, J., Grant, S.R. and Olson, E.N. (1998) A calcineurin-dependent transcriptional pathway for cardiac hypertrophy. *Cell*, **93**, 215–228.
34. Wilkins, B.J., Dai, Y.S., Bueno, O.F., Parsons, S.A., Xu, J., Plank, D.M., Jones, F., Kimball, T.R. and Molkentin, J.D. (2004) Calcineurin/NFAT coupling participates in pathological, but not physiological, cardiac hypertrophy. *Circ. Res.*, **94**, 110–118.
35. Rothermel, B.A., Vega, R.B. and Williams, R.S. (2003) The role of modulatory calcineurin-interacting proteins in calcineurin signaling. *Trends Cardiovasc. Med.*, **13**, 15–21.
36. Dorn, G.W. II and Force, T. (2005) Protein kinase cascades in the regulation of cardiac hypertrophy. *J. Clin. Invest.*, **115**, 527–537.
37. Palaniyandi, S.S., Sun, L., Ferreira, J.C. and Mochly-Rosen, D. (2009) Protein kinase C in heart failure: a therapeutic target? *Cardiovasc. Res.*, **82**, 229–239.
38. Churchill, E., Budas, G., Vallentin, A., Koyanagi, T. and Mochly-Rosen, D. (2008) PKC isozymes in chronic cardiac disease: possible therapeutic targets? *Annu. Rev. Pharmacol. Toxicol.*, **48**, 569–599.
39. Braun, M.U., LaRosee, P., Schon, S., Borst, M.M. and Strasser, R.H. (2002) Differential regulation of cardiac protein kinase C isozyme expression after aortic banding in rat. *Cardiovasc. Res.*, **56**, 52–63.
40. Bowling, N., Walsh, R.A., Song, G., Estridge, T., Sandusky, G.E., Fouts, R.L., Mintze, K., Pickard, T., Roden, R., Bristow, M.R. *et al.* (1999) Increased protein kinase C activity and expression of Ca2+-sensitive isoforms in the failing human heart. *Circulation*, **99**, 384–391.
41. Simpson, P.C. (1999) Beta-protein kinase C and hypertrophic signaling in human heart failure. *Circulation*, **99**, 334–337.
42. Wakasaki, H., Koya, D., Schoen, F.J., Jirousek, M.R., Ways, D.K., Hoit, B.D., Walsh, R.A. and King, G.L. (1997) Targeted overexpression of protein kinase C beta2 isoform in myocardium causes cardiomyopathy. *Proc. Natl Acad. Sci. USA*, **94**, 9320–9325.
43. Goldspink, P.H., Montgomery, D.E., Walker, L.A., Urboniene, D., McKinney, R.D., Geenen, D.L., Solaro, R.J. and Buttrick, P.M. (2004) Protein kinase Cepsilon overexpression alters myofilament properties and composition during the progression of heart failure. *Circ. Res.*, **95**, 424–432.
44. Takeishi, Y., Ping, P., Bolli, R., Kirkpatrick, D.L., Hoit, B.D. and Walsh, R.A. (2000) Transgenic overexpression of constitutively active protein kinase C epsilon causes concentric cardiac hypertrophy. *Circ. Res.*, **86**, 1218–1223.
45. Liang, X., Zhou, Q., Li, X., Sun, Y., Lu, M., Dalton, N., Ross, J. Jr. and Chen, J. (2005) PINCH1 plays an essential role in early murine embryonic development but is dispensable in ventricular cardiomyocytes. *Mol. Cell. Biol.*, **25**, 3056–3062.
46. Rodriguez, C.I., Buchholz, F., Galloway, J., Sequerra, R., Kasper, J., Ayala, R., Stewart, A.F. and Dymecki, S.M. (2000) High-efficiency deleter mice show that FLPe is an alternative to Cre-loxP. *Nat. Genet.*, **25**, 139–140.
47. O'Gorman, S., Dagenais, N.A., Qian, M. and Marchuk, Y. (1997) Protamine-Cre recombinase transgenes efficiently recombine target sequences in the male germ line of mice, but not in embryonic stem cells. *Proc. Natl Acad. Sci. USA*, **94**, 14602–14607.
48. Rungby, J., Kassem, M., Eriksen, E.F. and Danscher, G. (1993) The von Kossa reaction for calcium deposits: silver lactate staining increases sensitivity and reduces background. *Histochem. J.*, **25**, 446–451.
49. Chang, S., McKinsey, T.A., Zhang, C.L., Richardson, J.A., Hill, J.A. and Olson, E.N. (2004) Histone deacetylases 5 and 9 govern responsiveness of the heart to a subset of stress signals and play redundant roles in heart development. *Mol. Cell. Biol.*, **24**, 8467–8476.